

Supporting Information

For

Preparation of a poly (3'-azido-3'-deoxythymidine-co-propargyl methacrylate-co-pentaerythritol triacrylate) monolithic column by *in situ* polymerization and click reaction for capillary liquid chromatography of small molecules and proteins

Zian Lin,^{a,b*} Ruifang Yu,^a Wenli Hu,^a Jiangnan Zheng,^a Ping Tong,^a Hongzhi Zhao,^b and Zongwei Cai,^{b*}

a) Ministry of Education Key Laboratory of Analysis and Detection for Food Safety, Fujian Provincial Key Laboratory of Analysis and Detection Technology for Food Safety, College of Chemistry, Fuzhou University, Fuzhou, Fujian, 350116, China

b) Partner State Key Laboratory of Environmental and Biological Analysis, Department of Chemistry, Hong Kong Baptist University, 224 Waterloo Road, Kowloon Tong, Hong Kong, SAR, P. R. China

● **First corresponding author:** Zian Lin;

● **Second corresponding author:** Zongwei Cai

● **Postal address:** College of Chemistry, Fuzhou University,

Fuzhou, Fujian, 350116, China

● **Fax:** 86-591-22866135

E-mail: zianlin@fzu.edu.cn (Z.A. Lin); zwcai@hkbu.edu.hk (Z.W. Cai)

Table S1 Evaluation and comparison on the resolution and column efficiency of the poly(AZT-co-PMA-co-PETA) monolith, poly(PMA-co-PETA) monolith and AZT-modified poly(PMA-co-PETA) monolith.

Column	Parameters	Toluene	DMF	Formamide	Thiourea
Poly(AZT-co-PMA-co-PETA) monolith	N(plates/m)	38372	32468	47284	6720
	Rs	---	2.20	4.84	10.66
Poly(PMA-co-PETA) monolith	N(plates/m)		68616(overlap)		66508
	Rs		---		1.19
AZT-modified poly(PMA-co-PETA) monolith	N(plates/m)	19056	10432	11904	4589
	Rs	---	1.24	2.19	10.68

The experimental conditions were the same as in Fig. 4.

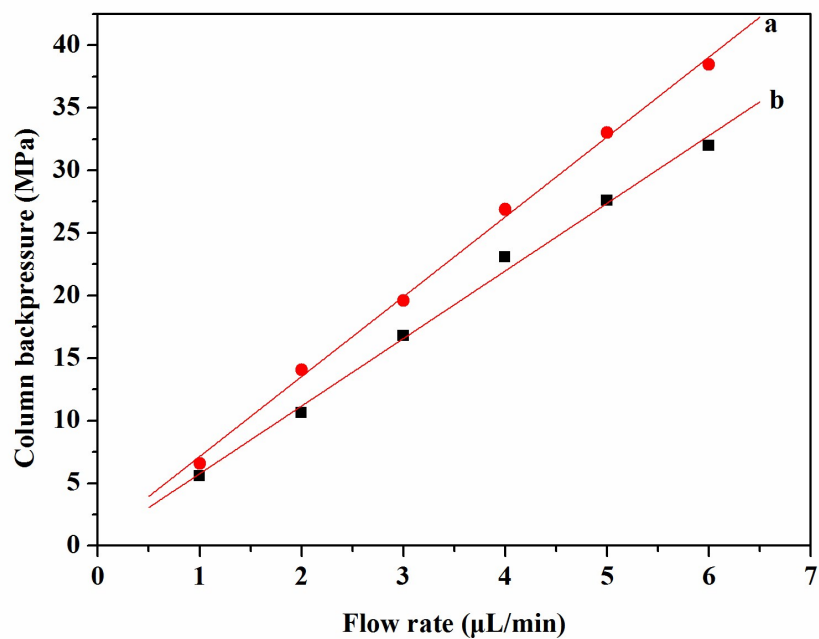


Fig.S1. Effect of mobile phase flow rate on column backpressure for poly(AZT-co-PMA-co-PETA) monolithic capillary column. Mobile phase: (a) water and (b) methanol.

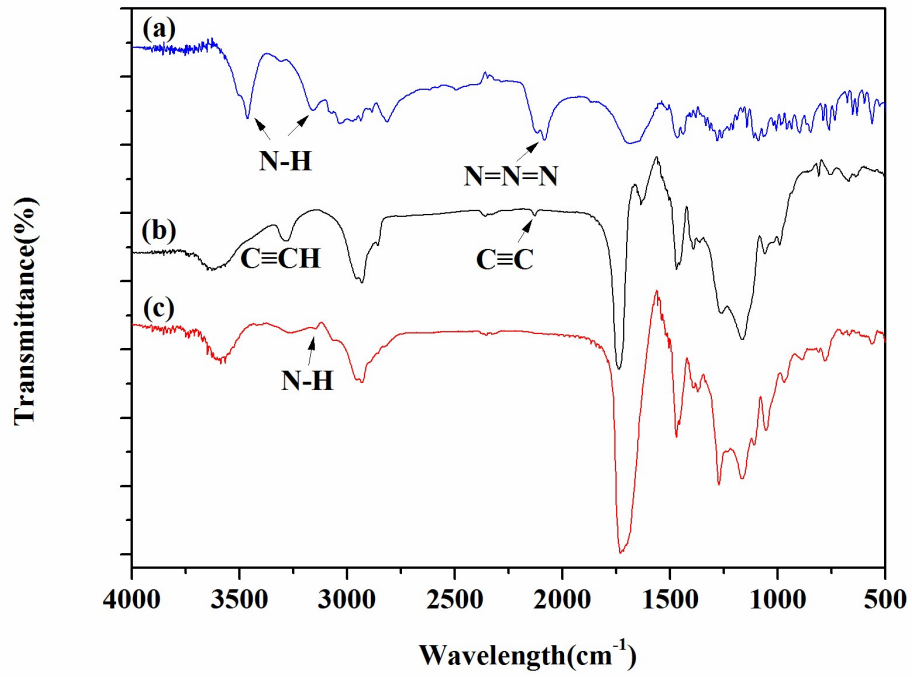


Fig.S2. FT-IR spectra of AZT (a), poly (PMA-co-PETA) monolith (b) and poly (AZT-co-PMA-co-PETA) monolith (c).

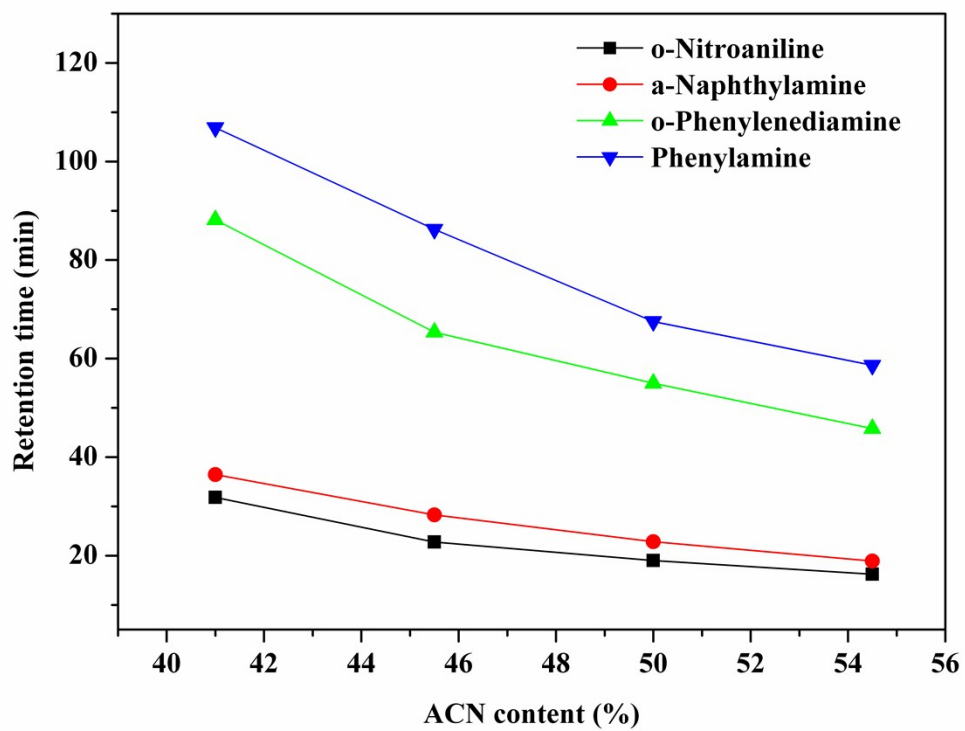


Fig.S3. Effect of ACN content on retention time of anilines on the poly (AZT-co-PMA-co-PETA) monolith.

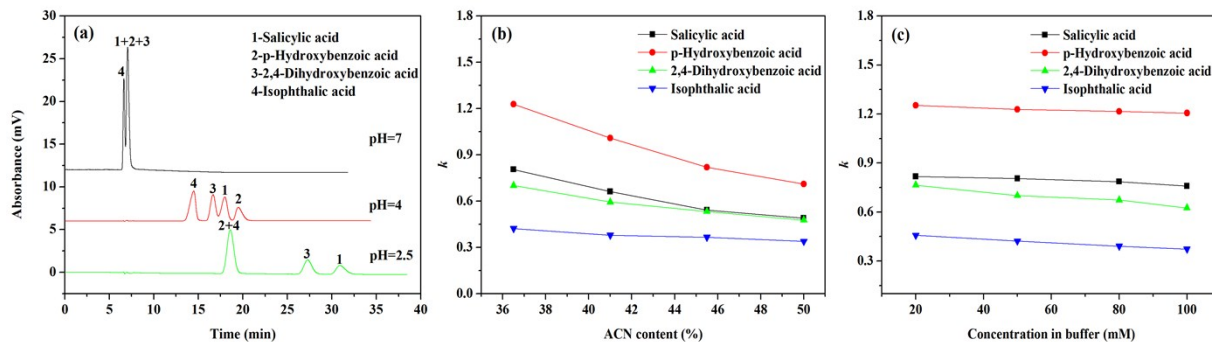
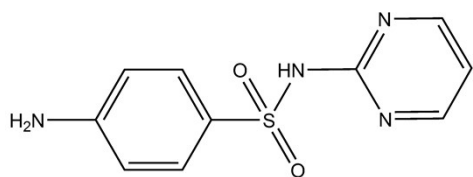
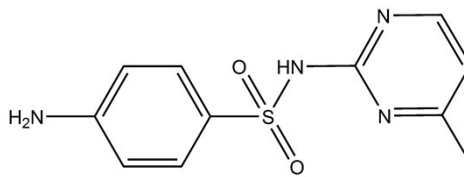


Fig.S4. (a) Anion-exclusion/ hydrophobic interaction chromatography for the separation of benzoic acids at varying pH, (b) effect of ACN content on the k' values of benzoic acids and (c) effect of salt concentration on the k' values of benzoic acids on the poly(AZT-co-PMA-co-PETA) monolith (column C).

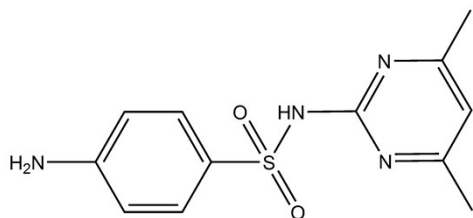
Conditions for (a): Mobile phase: 50 mM PB containing 36.5% (v/v) ACN with various pH; Pump pressure: 5.6 MPa; Flow rate (actual flow rate after splitting): 0.02 mL/min (80 nL/min); Detection wavelength: 214 nm; For (b) and (c), all the conditions are same as (a) except for pH 4.0; the analytes are (1) salicylic acid (100 ppm); (2) p-hydroxybenzoic acid (100 ppm); (3) 2,4-dihydroxybenzoic acid (100 ppm); (4) isophthalic acid (100 ppm).



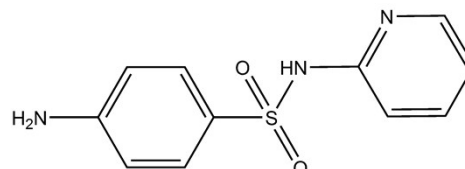
sulfadiazine (SDZ)



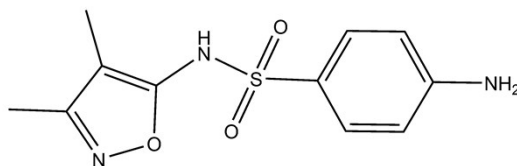
sulfamerazine (SMR)



sulfamethazine (SMZ)

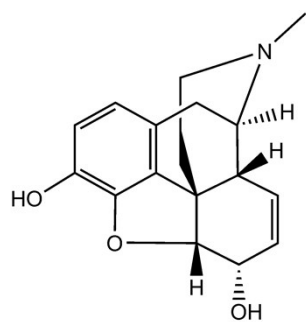


sulfapyridine (SPD)

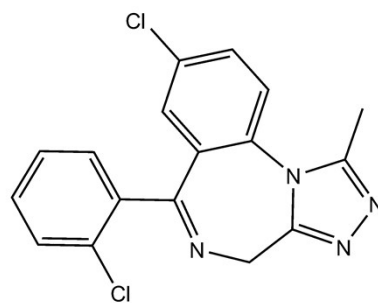


sulfisoxazole (SIZ)

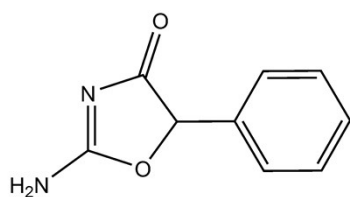
Fig.S5 Chemical structures of five sulfonamide antibiotics.



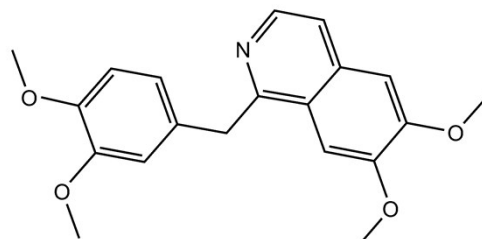
morphine



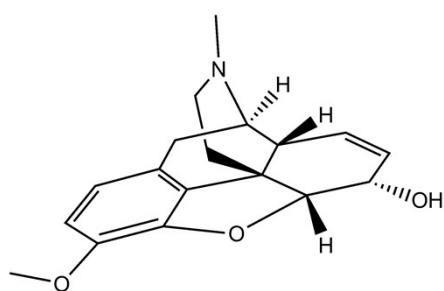
triazolam



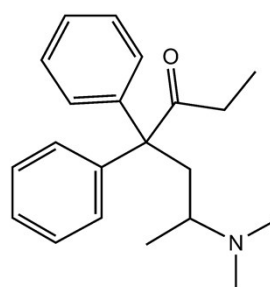
pemoline



papaverine

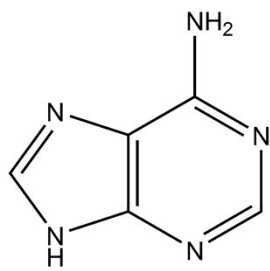


codeine

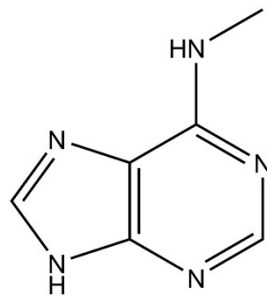


adanon

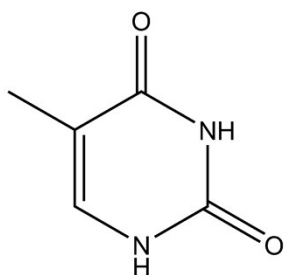
Fig.S6 Chemical structures of six anesthetics.



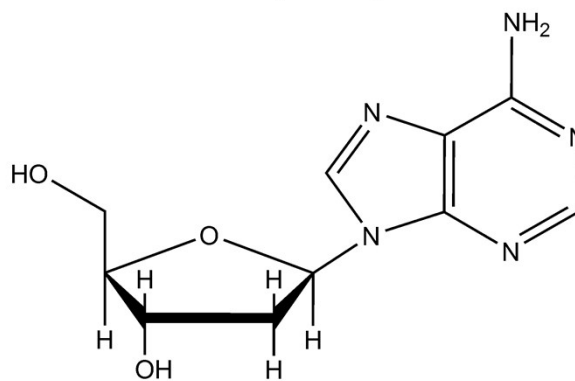
adenine



6-methylaminopurine



thymine



2-deoxyadenosine

Fig.S7 Chemical structures of four nucleosides and nucleobases.

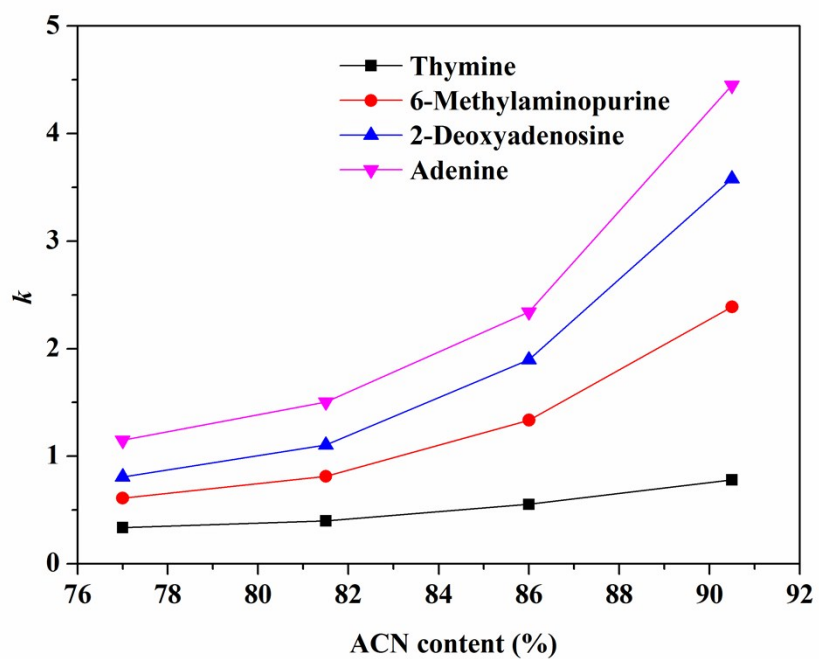


Fig.S8 Effect of ACN content on the k values of nucleosides and nucleobases on the poly (AZT-co-PMA-co-PETA) monolith (column C).